Supported Ni catalysts from nominal monolayer grow single-walled carbon nanotubes.

Kazunori Kakehi [a], Suguru Noda [a,*], Shohei Chiashi [b], Shigeo Maruyama [b]

[a] *Department of Chemical System Engineering, School of Engineering, The University of Tokyo, 7-3-1 Hongo, Bunkyo-ku, Tokyo 113-8656, Japan*
[b] *Department of Mechanical Engineering, School of Engineering, The University of Tokyo, 7-3-1 Hongo, Bunkyo-ku, Tokyo 113-8656, Japan*
Received 4 April 2006; in final form xx June 2006

Abstract

Fe, Co, and Ni are catalytically effective for growing single-walled carbon nanotubes (SWNTs). On substrates, however, Ni tends to yield only multi-walled carbon nanotubes. Because enhanced surface diffusion at the elevated growth temperature required for deposition might cause coarsening of Ni catalyst nanoparticles, adjusting the nominal Ni thickness should be crucial for controlling the particle size. Using our previously developed combinatorial method, we prepared a thickness profile of Ni on a quartz glass (SiO_2) substrate and found that Ni nanoparticles catalyzed the growth of SWNTs by chemical vapor deposition only when nominal thickness of Ni was in the monolayer range.

1. Introduction

Single-walled carbon nanotubes (SWNTs) have attracted much attention as promising materials for application in nanodevices due to their unique properties. To realize such applications, their controlled growth on various substrates is crucial. Although arc discharge [1] and laser ablation [2] have been used to grow SWNTs, chemical vapor deposition (CVD) with nanoparticle catalysts is now mainly used. Fe, Co, and Ni are catalytically effective. Fe and Co can grow SWNTs when they are suspended in the gas-phase [3,4] or supported on substrates [5,6]. However, Ni tends to grow only MWNTs when it is supported on substrates. Paillet et al. grew SWNTs; they prepared "discrete Ni catalyst nanoparticles" on SiO_2/Si substrates by spin-coating colloid-chemically synthesized Ni nanoparticles [7]. Their Ni nanoparticles (4.7 ± 1.4 nm) grew much thinner SWNTs (1.45 ± 0.5 nm) at a synthesis yield (i.e., number ratio of grown SWNTs to Ni nanoparticles) of less than 0.5 to 4%. Despite the rather large diameter and small areal density (40-100 nanoparticles/μm^2), the nanoparticles aggregated and grew large after CVD at 1223 K. Coarsening of Ni nanoparticles by the enhanced surface diffusion at the elevated CVD temperature is possibly why Ni tends to grow only MWNTs when supported on substrates.

Surface diffusion of catalyst metals can also be utilized to spontaneously form catalyst nanoparticles of a desirable size at the temperature required for CVD. The size of nanoparticles is determined by the amount of metals within the area of their surface diffusion, and thus the nominal thickness is the key parameter to control the particle size. Previously, we prepared a thickness profile of Co on a SiO_2/Si substrate by our *"combinatorial masked deposition (CMD)"* method [8], carried out alcohol catalytic CVD (ACCVD) [9], and grew high-quality SWNTs by Co nanoparticle catalysts spontaneously forming from nominal Co submonolayers [6]. Such tiny nanoparticles should reach an equilibrium shape, which is determined by the balance between surface energy of the deposit, that of the substrate, and

* Corresponding author: Fax: +81-3-5841-7332.

E-mail Address: noda@chemsys.t.u-tokyo.ac.jp (S. Noda).

their interfacial energy. When metals are deposited on oxides, their shapes can be explained by using the heats of sublimation and oxidation of metals in place of the energies of the metal surface and the metal/oxide interface, respectively [10]. Among Fe, Co, and Ni, the heats of sublimation are comparable, but the heats of oxidation decrease in that order. The poorest wettability, and thus the fastest surface diffusion, is expected for Ni.

To spontaneously form Ni nanoparticle catalysts on substrates, the nominal Ni thickness should be very small; if Ni forms nanoparticles of the same diameter as Co and grows SWNTs of the same diameter at the same synthesis yield as Co, the optimum thickness for Ni is expectedly smaller than for Co (around 0.1 nm) [6]. In this work, we applied our CMD method to discover the optimum Ni thickness for supported Ni catalysts to grow SWNTs.

2. Experimental

The detailed procedures for catalyst preparation and CVD were described elsewhere [6,11]. A thickness profile of Ni was prepared on a SiO_2 substrate in one direction by applying the CMD method with a slit-mask to r.f. magnetron sputtering [11]. The nominal thickness of Ni (t_{Ni}) varied from 0.05 to 3.5 nm, which was estimated by the deposition rate profile determined for thicker films by a surface profilometer. Then, the sample was exposed to air and set in a hot-wall tubular CVD reactor. The sample was heated to a target temperature of 1050 K under 4 vol% H_2/Ar flow at 2.7 kPa, kept at that temperature for 10 min, and ACCVD was carried out by flowing pure ethanol vapor at 1.3 kPa for 10 min. The samples were then characterized by using micro-Raman scattering spectroscopy (Seki Technotron, STR-250), field emission scanning electron microscopy (FE-SEM, Hitachi S-4700 and S-900), and transmission electron microscopy (TEM, JEOL 2000EX).

3. Results and discussion

Figure 1 shows typical Raman spectra for the carbon nanotubes (CNTs) grown on supported Ni substrates. For t_{Ni} = 3.5 nm (Fig. 1a), weak peaks were observed for the G-band (at ~ 1590 cm^{-1}) and D-band (at ~ 1350 cm^{-1}). For t_{Ni} < 1 nm (Figs. 1b-d), the spectra significantly differed; the G-band peak was sharp and branched, the D-band peak was very small, and peaks appeared for the radial breathing mode (RBM, around 150-280 cm^{-1}). These characteristics indicate that SWNTs were the main products. Note that the intensity of the RBM peaks was relatively small compared with that of the G-band because of the notch filter used in the measurement and because of the relatively small sensitivity of RBM of SWNTs around 2 nm or above, which were the main product as discussed later. The RBM peaks appeared at higher Raman shifts with decreasing t_{Ni}, indicating the growth of thinner SWNTs.

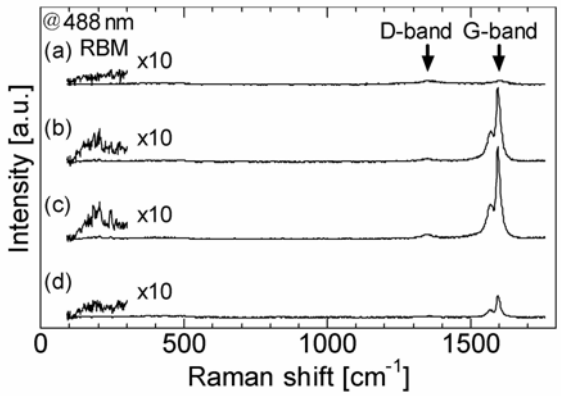

Fig. 1. Raman spectra of carbon nanotubes measured using 488-nm excitation. Nominal thicknesses of Ni (t_{Ni}) were (a) 3.5, (b) 0.46, (c) 0.22, and (d) 0.05 nm.

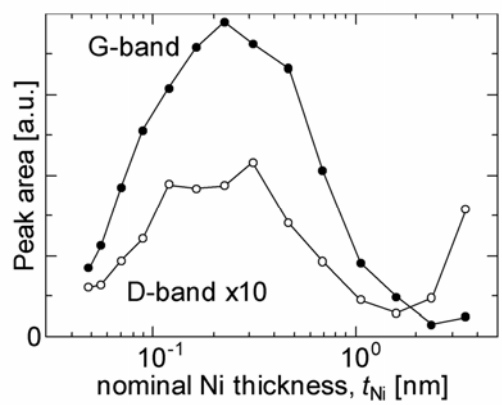

Fig. 2. Peak areas of the G- and D-bands of Raman spectra versus t_{Ni}. For easier comparison, the value for the D-band was multiplied by 10.

Figure 2 shows the peak areas of the G- and D-bands against t_{Ni}. As t_{Ni} decreased from 3.5 to 0.05 nm, the peak area of the G-band increased, reached a maximum at t_{Ni} = 0.22 nm, and then decreased. The peak area of the D-band changed similarly to that of the G-band except for t_{Ni} > 1 nm, and the peak area ratio of the G-band to D-band was ~ 20 for 0.07 < t_{Ni} < 1 nm. The largest intensity of the G-band was achieved for t_{Ni} = 0.22 nm under the ACCVD conditions of this work.

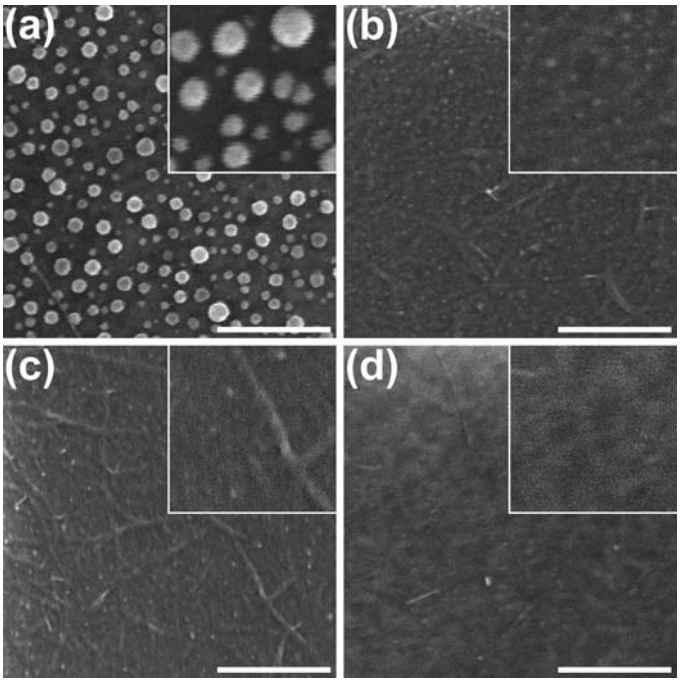

Fig. 3. Plan-view FE-SEM images of carbon nanotubes at the same t_{Ni} as (a)-(d) in Fig. 1. Scale bars are 200 nm. Insets show images at twice the magnification.

Figure 3 is plan-view FE-SEM images of the sample taken at the same positions as the Raman spectra (Fig. 1). At t_{Ni} = 3.5 nm (Fig. 3a), Ni particles with diameters larger than 10 nm were formed and few carbon nanotubes were observed. As t_{Ni} decreased, Ni particles became smaller and carbon nanotubes, presumably bundles of SWNTs, appeared and became

more pronounced (Figs. 3b,c). Further decrease in t_{Ni} made Ni particles unobservable and carbon nanotubes appeared to be thinner bundles or individual SWNTs (Fig. 3d).

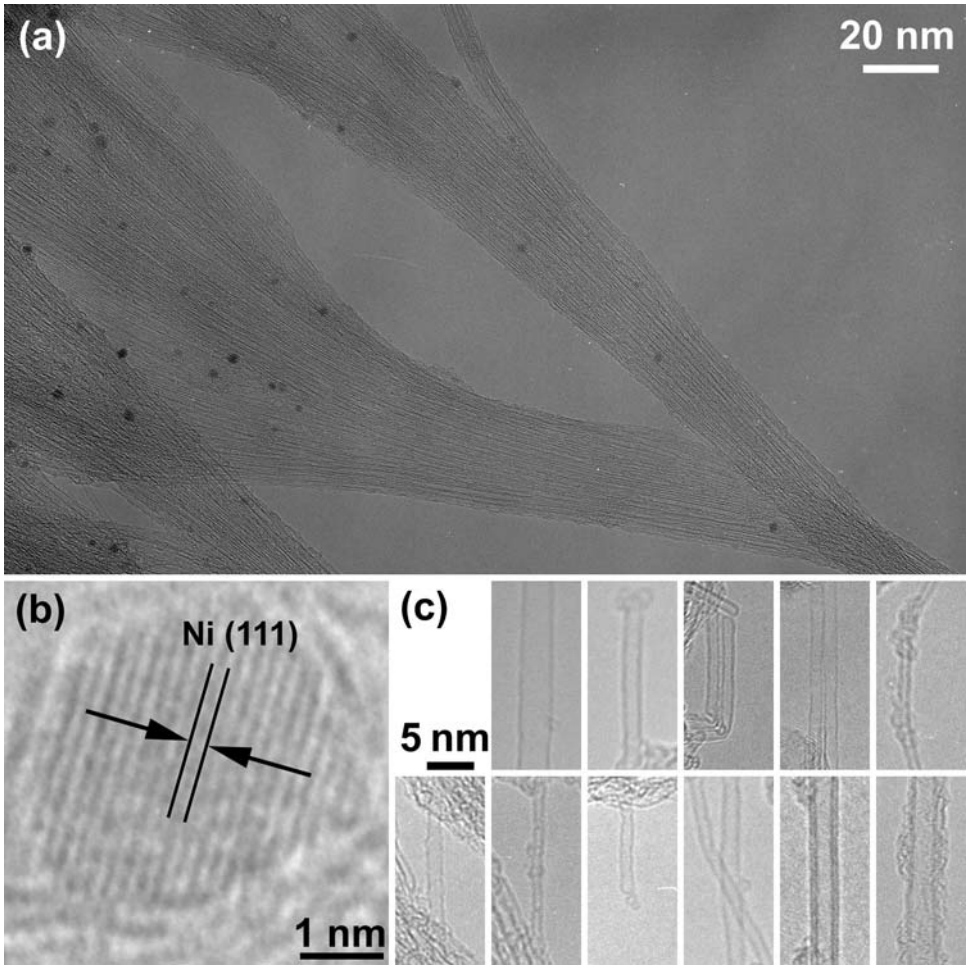

Fig. 4. TEM images of as-grown carbon nanotubes grown with uniform t_{Ni} = 0.22 nm. (a) CNT bundles, (b) lattice image of Ni nanoparticles, and (c) individual CNTs. The lattice constant of the Ni (111) plane is 0.203 nm.

Figure 4a shows TEM images of the as-grown CNTs grown on another SiO_2 substrate with uniform t_{Ni} = 0.22 nm. Thick and thin bundles of carbon nanotubes were observed as well as some amorphous carbon and nanoparticles. The lattice image (Fig. 4b) indicates that these nanoparticles were Ni. More catalyst nanoparticles were observed for this sample than that grown by Co catalysts [8]. This is possibly due to the poorer wettability of Ni than Co on SiO_2 surfaces, which resulted in lift-off of Ni nanoparticles from the substrate. Figure 4c shows typical TEM images of individual CNTs. The diameters of the CNTs ranged from 1.2 to 4.6 nm and the average diameter was 2.2 nm. About 80% of the CNTs were SWNTs, the remaining CNTs were double-walled, and no MWNT with more than three layers was observed. In summary, Ni supported on substrates catalyzed the growth of SWNTs when its nominal thickness was as thin, namely, in the monolayer range.

Contrary to our prediction, the optimum thickness for the SWNTs growth was somewhat larger for Ni (~ 0.2 nm) than for Co (~ 0.1 nm) [6]. Furthermore, the thicker Ni grew a much smaller amount of SWNTs than did Co [6]. We discuss the reason for this result by considering the relationship between the diameter and areal density of SWNTs and those

of Ni nanoparticles. First, we describe the diameter and areal density of SWNTs. Based on the TEM images (Fig. 4c), many SWNTs had diameters around 2 nm. In the FE-SEM image (Fig. 3c), these SWNTs formed bundles whose diameter was ~ 10 nm and areal density was 2.8×10^2 bundles/μm^2. The number of SWNTs per bundle was about 10~ 100, and thus the areal density of SWNTs was estimated at around 10^4 SWNTs/μm^2. Next, we discuss the diameter and areal density of Ni nanoparticles. We prepared samples with t_{Ni} = 0.22 nm and observed the nanoparticles by SEM without growing SWNTs. No particles were observed for the as-sputtered sample (Fig. 5a), probably because the Ni particles were too small to be observed by SEM. After annealing at 1050 K for 10 min under 4 vol% H_2/Ar flow, Ni particles were clearly observed (Fig. 5b). These results show that the surface diffusion process at the CVD temperature dominates the diameter and areal density of the Ni catalyst nanoparticles. Figure 5c shows the size distribution of the Ni particles obtained from the TEM and SEM images. The shape was similar for these distributions, but the size was somewhat different. The average diameter was larger for the SEM observation (5.3 ± 0.8 nm) than for the TEM observation (4.4 ± 0.6 nm), possibly due to the poorer spatial resolution of SEM than TEM. The areal density of the Ni particles was 1.0×10^4 nanoparticles/μm^2, similar to the estimated areal density of SWNTs, suggesting that most Ni particles were catalytically active to grow SWNTs. Cross-sectional FE-SEM images of larger Ni particles (≥ 10 nm) at t_{Ni} = 3.5 nm (not shown here) showed that Ni nanoparticles were hemispherical. If we assume that Ni nanoparticles were hemispheres whose areal density was 1.0×10^4 nanoparticles/μm^2 and diameter was 4.4 nm, their nominal thickness becomes 0.22 nm. This value is consistent with the amount of Ni supplied, and therefore, the diameter and areal density of Ni particles would be reliable. Because the size of Ni particles apparently increases with t_{Ni} (Fig. 3), the largest SWNT yield at t_{Ni} = 0.22 nm shows that 4-5-nm-sized Ni particles had the largest catalytic activity in growing 2-nm-diameter SWNTs under the CVD condition of this work.

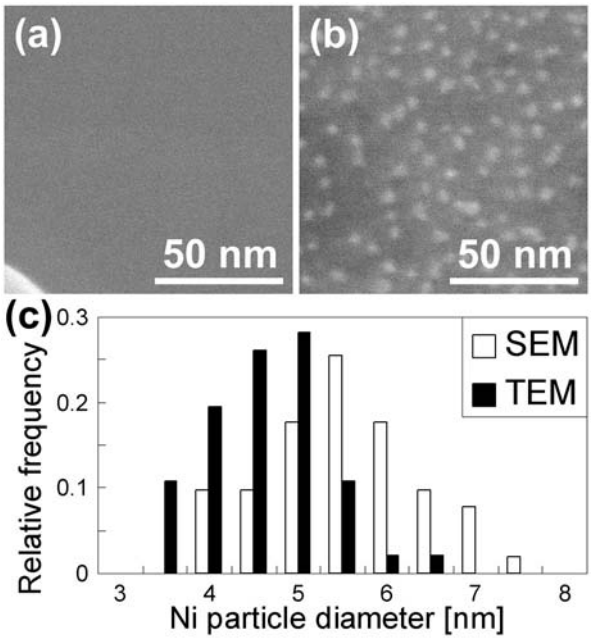

Fig. 5. Plan-view FE-SEM image of Ni particles (a) before and (b) after annealing at 1050 K and t_{Ni} = 0.22 nm. The object at the bottom-left corner of (a) is a dust particle used for focus adjustment. (c) Size distributions of Ni particles obtained from TEM and SEM images.

The larger diameter of Ni particles than that of SWNTs might be an origin for the thicker optimum thickness for Ni than for Co. Paillet et al. made similar observations [7], and reported also for Fe [12-14] on a similar discrepancy. Possible reasons for this discrepancy include particle-trapping process [12], amorphous carbon formation on the catalyst during cooling [13], and formation of a junction between a spherical surface of graphene on the catalyst particle and the cylindrical surface of CNT [14]. The first two mechanisms (particle-trapping process and amorphous carbon formation) cannot explain our results, because Ni nanoparticles before and after ACCVD (Figs. 4a and 5b) had nearly the same size. The third mechanism (formation of a junction) might be applicable to our results, although this needs verification. However, the discrepancy of diameters of Ni nanoparticles and SWNTs cannot fully explain the poorer catalytic activity of Ni than Co. From the FE-SEM images, the SWNT bundles grown by Ni (Fig. 3c) were apparently shorter than those grown by Co [6], indicating easier deactivation of Ni than Co. Moreover, the discrepancy in diameter between the catalyst and SWNTs may also be explained by easier deactivation: Thinner SWNTs are grown from a limited area of catalyst surfaces, namely, an area not covered by carbon. We need a further study to obtain a direct proof of this explanation.

As for the upper limit of the Ni particle diameter, it may be correlated with the melting temperature of these particles. The melting temperature of 4-5-nm-sized Ni particles decreases as low as 1050-1120 K [15], which agrees with the CVD temperature of this work. The larger Ni particles are in the solid state, and this is possibly the reason why the larger Ni particles were catalytically less active. There is an uncertainty; we also need to consider the effect of carbon concentration in Ni particles on their melting temperature. We are now investigating the effect of the CVD temperature on the optimum diameter of Ni catalyst particles.

4. Conclusions

Ni is an effective catalyst for the growth of SWNTs. When supported on substrates, however, Ni seldom grows SWNTs. Here, we screened the nominal thickness of Ni for a relatively wide range (0.05-3.5 nm) on SiO_2, and found that Ni nanoparticles catalyzed the growth of SWNTs by ACCVD only when its nominal thickness was in the monolayer range. The yield of SWNTs was much smaller for Ni than for Co, although the optimum metal thickness was somewhat larger for Ni (~ 0.2 nm) than for Co (~ 0.1 nm). Ni nanoparticles (4-5 nm) catalyzed the growth of thinner SWNTs (~ 2 nm); this possibly explains the larger optimum metal thickness for Ni than for Co. The melting temperature of 4-5-nm-sized Ni particles agreed with the CVD temperature of this work, suggesting that the catalyst particles were in the liquid phase and their optimum size depends on the CVD conditions, especially on temperature.

Acknowledgements

The authors thank Messrs. T. Osawa, H. Tsunakawa, and K. Ibe for their assistance in TEM observations. This work was financially supported in part by JSPS and NEDO of Japan.

References

[1] S. Iijima, T. Ichihashi, Nature 363 (1993) 603.
[2] T. Guo, P. Nikolaev, A. Thess, D.T. Colbert, R.E. Smalley, Chem. Phys. Lett. 243 (1995) 49.
[3] P. Nikolaev, M.J. Bronikowski, R.K. Bradley, F. Rohmund, D.T. Colbert, K.A. Smith, R.E. Smalley, Chem. Phys. Lett. 313 (1999) 91.
[4] T. Saito, S. Ohshima, W.-C. Xu, H. Ago, M. Yumura, S. Iijima, J. Phys. Chem. B 109

(2005) 10647.
[5] Y. Homma, T. Yamashita, P. Finnie, M. Tomita, T. Ogino, Jpn. J. Appl. Phys. 41 (2002) L89.
[6] S. Noda, Y. Tsuji, Y. Murakami, S. Maruyama, Appl. Phys. Lett. 86 (2005) 173106.
[7] M. Paillet, V. Jourdain, P. Poncharal, J.L. Sauvajol, A. Zahab, J.C. Meyer, S. Roth, N. Cordente, C. Amiens, B. Chaudret, J. Phys. Chem. B 108 (2004) 17112.
[8] S. Noda, Y. Kajikawa, H. Komiyama, Appl. Surf. Sci. 225 (2004) 372.
[9] S. Maruyama, R. Kojima, Y. Miyauchi, S. Chiashi, M. Kohno, Chem. Phys. Lett. 360 (2002) 229.
[10] M. Hu, S. Noda, H. Komiyama, Surf. Sci. 513 (2002) 530.
[11] S. Noda, H. Sugime, T. Osawa, Y. Tsuji, S. Chiashi, Y. Murakami, S. Maruyama, Carbon 44 (2006) 1414.
[12] G.-H. Jeong, A. Yamazaki, S. Suzuki, Y. Kobayashi, Y. Homma, Chem. Phys. Lett. 422 (2006) 83.
[13] S. Huang, M. Woodson, R. Smalley, J. Liu, Nano Lett. 4 (2004) 1025.
[14] A.G. Nasibulin, P.V. Pikhitsa, H. Jiang, E.I. Kauppinen, Carbon 43 (2005) 2251.
[15] A. Moisala, A.G. Nasibulin, E.I. Kauppinen, J. Phys.: Condens. Matter 15 (2003) S3011.